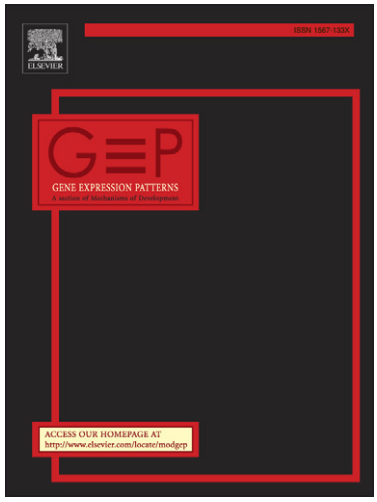

Gene expression analysis of canonical Wnt pathway transcriptional regulators during early morphogenesis of the facial region in the mouse embryo

Victor Vendrell, Kristen Summerhurst, James Sharpe, Duncan Davidson, Paula Murphy

PII: S1567-133X(09)00043-X
DOI: 10.1016/j.gep.2009.03.001
Reference: MODGEP 677

To appear in: *Gene Expression Patterns*

Received Date: 29 August 2008
Revised Date: 24 February 2009
Accepted Date: 9 March 2009

Please cite this article as: Vendrell, V., Summerhurst, K., Sharpe, J., Davidson, D., Murphy, P., Gene expression analysis of canonical Wnt pathway transcriptional regulators during early morphogenesis of the facial region in the mouse embryo, *Gene Expression Patterns* (2009), doi: 10.1016/j.gep.2009.03.001

Gene expression analysis of canonical Wnt pathway transcriptional regulators during early morphogenesis of the facial region in the mouse embryo

Victor Vendrell[1,4], Kristen Summerhurst[1], James Sharpe[3], Duncan Davidson[2] and Paula Murphy[1]*

1. Department of Zoology, School of Natural Sciences, Trinity College Dublin, Ireland.
2. MRC Human Genetics Unit, Western General Hospital, Crewe Road, Edinburgh EH6 2XU, Scotland
3. ICREA, EMBL-CRG Systems Biology Unit, Centre for Genomic Regulation, UPF, Dr. Aiguader 88, 08003, Barcelona, Spain
4. Present address, Conway Institute, University College Dublin.

*Address for correspondence: Paula Murphy, Department of Zoology, Trinity College Dublin, Ireland, Phone: +353-1-896-3780; Fax: +353-679-; E-mail: paula.murphy@tcd.ie.

Abstract

Structures and features of the face, throat and neck are formed from a series of branchial arches that grow out along the ventrolateral aspect of the embryonic head. Multiple signaling pathways have been implicated in patterning interactions that lead to species specific growth and differentiation within the branchial region that sculpt these features. A direct role for Wnt signaling in particular has been shown. The spatial and temporal distribution of Wnt pathway components contributes to the operation of the signaling system. We present the precise distribution of gene expression of canonical Wnt pathway transcriptional regulators, Tcf1, Lef1, Tcf3, Tcf4 and β-catenin between embryonic day (E) 9.5 and 11.5. In situ hybridization combined with Optical Projection Tomography was used to record and compare distribution of transcripts in 3D within the developing branchial arches. This shows widespread yet very specific expression of the gene set indicating that all genes contribute to proper patterning of the region. Tcf1 and Lef1 are more prominent in rostral arches, particularly at later ages, and Tcf3 and Tcf4 are in general expressed more deeply (medial/endodermal aspect) in the arches than Tcf1 and Lef1. Comparison with Wnt canonical pathway readout patterns shows that the relationship between the expression of individual transcription factors and activation of the pathway is not simple, indicating complexity and flexibility in the signaling system.

Results and Discussion

The branchial arches (also known as pharangeal or visceral arches) are prominent features of vertebrate embryos appearing as a series of paired bulging outgrowths along the ventrolateral head. Initially relatively simple in structure with an external covering of ectoderm, an internal lining of endoderm and a mesenchymal core made up of lateral mesoderm and neural crest cells, this apparent simplicity belies a huge complexity of patterning events that give rise to intricate structures and features of the face, throat and neck. The first arch gives rise to the jaw and mastication musculature and the second arch to the hyoid and the muscles giving expression to the face. The resident lateral mesoderm gives rise to musculature, migrating neural crest cells to skeletal and connective tissues and the endoderm to glands of the pharynx.

Generation of facial shape depends on the spatial distribution of cellular processes in the facial primordia which consist of the medial and lateral nasal processes, in addition to the maxillary and mandibular processes of the first branchial arch. A crucial period in the patterning of these territories follows the influx of neural crest cells, prior to cellular differentiation, when species-specific changes in the size and shape of the primordia occur. Over the time period considered in this study (Embryonic day (E) 9.5-11.5), the primordia enlarge and fuse in a pattern that has been well defined, at least for the chick (reviewed in Jiang et al., 2006). Correct fusion is an important event and slight alterations in growth and patterning of the mesenchyme or epithelia can lead to cleft lip and palate (CLP) (Gorlin et al., 2001).

The patterning of facial primordia involves interplay between a prepattern carried by the neural crest cells as they migrate ventrally from the neural plate and resident patterning mechanisms within the branchial region. Particularly neural crest cells arising from the segmented hindbrain (Lumsden and Keynes, 1989; Murphy et al., 1989; Murphy and Hill, 1991; Wilkinson et al., 1989) express a Hox code (reviewed in Graham et al., 2004; Graham and Smith, 2001; Helms et al., 2005) and have been shown to carry a positional prepattern (Hunt et al., 1991; Schneider and Helms, 2003); however resident branchial patterning mechanisms are also involved (Grammatopoulos et al., 2000; Veitch et al.,

1999). There is evidence of early patterning information being generated in the ectoderm (Couly and Le Douarin, 1990; Ferguson et al., 2000; Hu et al., 2003) and the endoderm (reviewed in Begbie et al., 1999; Couly et al., 2002; Graham, 2001; Maden et al., 1996; Wendling et al., 2000).

Later stages of facial mophogenesis are driven by mesenchymal proliferation (McGonnell et al., 1998) guided by signals from facial epithelia (Wedden, 1987) and signals from mesenchyme also influence ectoderm (reviewed in (Francis-West et al., 1998). Multiple pathways are implicated in complex interactions and interregulatory mechanisms involving RAR signalling, BMPs, FGFs, Shh and Wnts. A direct role of Wnt signalling was shown (Juriloff et al., 2006) by mapping a recessive mutation that caused CLP to the linked genes Wnt3 and 9b. Nonsense mutations in WNT3 were associated with tetra-amelia (complete absence of limbs and CLP)(Niemann et al., 2004) and a targeted mutation in Wnt9b can cause kidney defects and CLP(Carroll et al., 2005). In a recent study, Brugmann et al. (2007) described regions of canonical Wnt responsiveness in mouse and chick embryo facial regions, showing a correlation with respective species-specific regions of outgrowth, and showed that outgrowth is altered following experimental disturbance of Wnt signalling.

It is clear that facial morphogenesis involves dialogue between different tissues expressing different molecules and there is a need to integrate detailed information at several levels to understand the networks involved. One level at which detailed information needs to be gathered is the level of gene expression and this study presents a series of expression patterns to begin such a compilation. Wnt signalling is essential for regional specification of the face and the differential distribution of pathway components must drive the precise localisation of Wnt signalling events. The nuclear effectors of canonical Wnt signalling are the Tcf/Lef family of transcription factors and the necessary co-activator β-catenin that converts Tcfs from repressors to activators (Clevers, 2006). While this paper focuses on expression of the genes encoding canonical Wnt pathway transcriptional regulators, the patterns have been analysed and compiled with a view to future integration with genes encoding other molecules involved in Wnt signalling

(Summerhurst et al., 2008) as well as components of cross interacting pathways. A recent initiative through the Edinburgh Mouse Atlas of Gene Expression (EMAGE) catalogues expression patterns of genes with possible roles in craniofacial development (Facebase).

We have previously reported the expression patterns of Wnt and Fzd genes in the mouse embryo at a single stage of development highlighting our approach that emphasises the importance of comprehensive descriptions in 3D, allowing integration and comparison across multiple genes (Summerhurst K. et al., 2008). Here we report detailed 3D expression analysis using Optical Projection Tomography (OPT)(Sharpe et al., 2002, Summerhurst K. et al., 2008) of the Tcf/Lef family of transcription factors and the co-regulator β-catenin across developmental time, E9.5 to E11.5, specifically in the facial primordia and lower branchial arches.

Figure 1 shows still images of 3D reconstructions following OPT of Tcf1, Lef1, Tcf3, Tcf4 and β-catenin expression patterns in whole embryos at E9.5, E10.5 and E11.5. Full 3D representations and series of virtual sections are available to view on a dedicated web site (www.tcd.ie/Zoology/research/WntPathway) and to download from the Edinburgh Mouse Atlas of Gene Expression (genex.hgu.mrc.ac.uk/Emage/database). Superficial views of expression in the facial region following whole mount in situ hybridisation (Fig 2) show that all genes are expressed in specific restricted territories in some cases varying with time, during facial patterning. But this Figure also highlights the fact that only limited detail is visible in these conventional external views.

To analyse and compare the patterns in more detail, 3D reconstructions of stage-matched embryos were virtually sectioned in comparable sagittal, transverse and coronal planes. Figures 3-5 compare the patterns at E9.5, figures 6-8 at E10.5 and figures 9-11 at E11.5. Table 1 summarises the expression of each gene in each territory and indicates the figure elements where a direct visual comparison can be made of the spatial distribution of transcripts.

At E9.5 branchial arches 1 and 2 are very prominent pairs of dumbbell shaped outgrowths. The outgrowth of arch 1 will largely form the mandibular component at later stages; the maxillary component is more inconspicuous at this stage. As at later ages and previously described (Galceran et al., 1999; Oosterwegel et al., 1993) the expression of Lef1 and Tcf1 is similarly distributed. However while Tcf1 is more widely and intensely expressed in the nasal region (Figs. 4b2, 5a2), Lef1 is more extensive in the anterior maxillary and mandibular components of branchial arch 1 (Fig. 3a2, 4c1, 5b1). Tcf3 is most strongly expressed in the nasal processes (Fig. 3c1, 4b3, 5a3) but is also detected throughout the region, whereas Tcf4 is most prominent in the mandibular component of the 1st branchial arch (Fig. 3d1, 4c4, 5b4). In the nasal processes Tcf4 is restricted to the medial region (Fig. 5a4). A striking feature of the Lef1 and Tcf1 pattern is elevated expression in the anterior of mandibular branchial arch 1 and the posterior of branchial arch 2 (Fig. 3a,b). This opposing polarity is not seen with Tcf3, which is more widely distributed with a slight proximo-distal gradient (Fig 4c3 and d3), and Tcf4 which is more at the core of the arch mesenchyme (Fig. 3d2, 4c4). The highest expression of Tcf4 is seen at the interface between the maxillary and mandibular components of branchial arch 1 (Fig 4.c4), a pattern that becomes more obvious at later stages. β-catenin is expressed in each of the primordia but shows gradients peaking at the lateral or distal margins (Fig. 3e2, 4a5-4e5, 5a5-5d5). The expression of β-catenin across the stages was found to be very dynamic, with elevated expression overlapping with Tcf/Lef genes in a complex manner. From external lateral views the pattern appears to overlap extensively with Lef1 and Tcf1 in the nasal process and branchial arches 1 and 2 but on analysis of serial sections the patterns show some differences (e.g. Fig. 4 columns a and c where β-catenin expression is more lateral).

Tcf1 is expressed also in the lateral aspects of the third and the newly formed fourth branchial arch while we only detected expression of Lef1 in branchial arch 3 and not 4 (Fig 5d1, 5d2 and not shown). The expression of Tcf1 in branchial arch 3 is consistently stronger than Lef1 (compare Fig 5d1 and d2).

At E10.5 the maxillary component of the 1st branchial and the 3rd branchial arch have become more prominent and the 4th and 6th arches are more clearly visible so the full

territorial arrangement of the facial and branchial region is most obvious at this stage. Tcf1 and Lef1 continue their polarised expression in the mandibular component of the 1st arch (anterior) and in the 2nd arch (posterior, distal). However expression is now extensive in the 3rd arch but clearly localised to the distal part, distal to the arch artery, and is detectable in the area of the 4th but not in the 6th arch (Fig. 8e1 and e2, Fig. 7e1 and 2). Tcf3 is now very widely expressed in the 2nd, 3rd, 4th and 6th arches and shows no such localisation to distal regions but is expressed deeply through the arches (Fig 8e3). In comparison to E9.5, Tcf3 expression becomes much more sharply defined at this later stage, particularly in the nasal process where it is expressed all around the nasal grooves (Fig 7a3 and Fig 8a3). Whereas there appeared to be a proximal-distal gradient of expression earlier, expression is now most intense in the core mesenchyme of branchial arches 1 and 2 (Fig 8b3 and c3).

Tcf4 at the same time point has become more localised to the opposing aspects of the mandibular and maxillary components of the 1st arch that will form the opposing upper and lower jaw lines. This overlaps with β-catenin expression in both regions and with Lef1 and Tcf1 expression in the maxillary component but not in the mandibular component. Expression of Tcf4 is still not detected in arches 2 and 3 but can now be seen on the medial side of the 4th arch artery (Fig. 7e4, 8e4).

At E10.5 β-catenin expression shows similarities to Tcf1 and Lef1 expression in branchial arches 1 and 2. In more rostral arches β-catenin shows an interesting pattern; throughout the 3rd arch, localised to the endodermal (proximal) part of the 4th arch and again more widespread in the region of the 6th arch (Fig 8e5). Figure 8 shows similarities in the territories of Tcf3 and β-catenin in arches 3-6.

At E11.5 growth of the arches and nasal processes has led to a tighter arrangement and relationship between the primordia and local fusion has commenced. Tcf1 and Lef1 still show similar patterns in the upper arches but Lef1 is more extensive in the mandibular component and Tcf1 is more extensive in the nasal processes (Fig 9). Tcf3 is very highly expressed in the mesenchyme of a more rostral domain in the nasal processes and is excluded from the nasal epithelia (Fig. 10a3). Tcf3 is most widely expressed throughout

the region. Tcf4 has become very localised and specific to the opposing posterior and anterior faces of the mandibular and maxillary processes (respectively) and to the very distal nasal region. β-catenin mirrors most closely this localised pattern of Tcf4 but also shows expression in the lateral maxillary component where Tcf1 and Lef1 are expressed. The earlier expression of Tcf4 in the 4th and 6th arches has now become more prominent around the branchial and pulmonary arteries with less expression of Tcf3 and β-catenin in this region (Fig. 11e).

Figures 3-11 and the 3D data downloadable through EMAGE display details of the expression patterns that cannot all be discussed here. However a number of general observations about the patterns can be made. All Tcf/Lef genes and β-catenin are expressed in all branchial arch territories in some tissue or stage suggesting that all contribute to the proper patterning of the branchial region (Table 1). Particularly at E10.5 when the full complement of branchial territories is most visible, the widespread yet very specific expression of this set of genes is obvious. Within the family Tcf1 and Lef1 show most similarities in expression but comparable sections in different orientations show significant differences in the distribution of transcripts. In general Tcf1 and Lef1 are expressed most extensively in rostral arches with lower level expression in caudal regions. This is most obvious at later ages when Tcf1 and Lef1 appear to be down-regulated in caudal arches. Tcf3 is most widely expressed and Tcf4 most restricted. Looking across branchial arches 2-6 at E10.5 (Fig 8, rows d and e) a trend is seen where Tcf1 and Lef1 are expressed in more lateral territories while Tcf3 extends and Tcf4 is localised to deeper tissues. Taking branchial arch 3 in particular to illustrate this, it is clear that Tcf1 and Lef1 are not expressed in or close to the endodermal aspect while Tcf3 and 4 are. β-catenin at this stage shows an interesting arch specific pattern with expression throughout the lateromedial extent of some arches and elevated in the medial/endodermal aspect in others.

These patterns will form part of a Wnt pathway specific 3D database which is under construction where detailed comparisons can be made across components. Comparing the expression patterns here with the patterns reported for canonical Wnt pathway readout in the branchial region (Brugmann et al 2007), very strong readout signal was seen in

proximal arch 1 at E9.5, in the lateral and medial but not the frontal nasal processes and in maxillary and mandibular arch 1 at E10.5, around the nasal pits and extensively in the maxillary component at E11.5 (compare Fig. 11 B with Fig. 11 columns a and c). Although aspects of the pattern appear quite similar to Tcf1, particularly at E11.5 (Fig 1) it is clear that there is not a simple relationship between the expression of individual transcription factors and activation of canonical signalling. This is reinforced by the complex relationship between elevated expression of β-catenin and the Tcf/Lef family genes shown here.

Supplementary data:

Movies of whole embryos representing each of the gene expression patterns are available on a dedicated web site http://www.tcd.ie/Zoology/research/WntPathway/ and full 3D reconstructed data are available to download from Edinburgh Mouse Atlas Gene Expression database EMAGE (genex.hgu.mrc.ac.uk/Emage/database) under the following accession numbers

Tcf1 E9.5: EMAGE:5765

Tcf1 E10.5: EMAGE:5759

Tcf1 E11.5: EMAGE:5760

Lef1 E9.5: EMAGE:5753

Lef1 E10.5: EMAGE:5757

Lef1E11.5: EMAGE:5758

Tcf3 E9.5: EMAGE:5766

Tcf3 E10.5: EMAGE:5761

Tcf3 E11.5: EMAGE:5762

Tcf4 E9.5: EMAGE:5754

Tcf4 E10.5: EMAGE:5763

Tcf4 E11.5: EMAGE:5764

βcatenin E9.5: EMAGE:5752

βcatenin E10.5: EMAGE:5755

βcatenin E11.5: EMAGE:5756

2. Experimental Procedures:

Probes: Details of the probes used to generate the data presented for each of the genes is shown in Table 2.

Embryo collection: Embryos were collected from time-mated CD1 females on the morning of the 10^{th}, 11^{th} or 12^{th} day following detection of a vaginal plug (E9.5, E10.5 or E11.5). Embryos typical of these embryonic days (Kaufman 1992) were selected for comparison across genes.

In Situ Hybridisation (ISH): The protocol used was largely as per Xu and Wilkinson (Xu and Wilkinson, 1998), optimised for OPT visualisation as described in Summerhurst et al. (2008). A minimum of two independent hybridisations with 5 embryos per probe were carried out for each gene where the expression patterns were very clear; for more difficult patterns up to 6 hybridisations were carried out often altering the probe being used. Each hybridisation included a sense control probe and Fgf8 (Crossley and Martin, 1995) as a standard by which to judge consistency across experiments.

Expression was revealed by colourometric stain using 175 µg/ml 4-Nitro blue tetrazolium chloride and 62.5 µg/ml 5-Bromo-4-chloroindolyl-phosphate with moderate staining intensity closely selected as described in Summerhurst et al (2008).

OPT scanning and 3D reconstruction: After photographing the wholemount data, at least two perfectly intact specimens from each hybridisation, representative of the externally visible pattern, were selected for OPT scanning (Sharpe et al., 2002). Scanning was carried out as described in Summerhurst et al. (2008). The raw data (400 projected images) from each of the scans were loaded onto a Linux workstation, reconstructed using a set of programmes provided by the Edinburgh Mouse Atlas Project (EMAP) and analysed using custom made software (MA3DView and MAPaint), again provided by EMAP.

To focus on expression in the facial region, full reconstructions were digitally cropped for detailed comparison. Expression patterns were compared crudely by viewing the volume rendered data externally and in detail by viewing matching section planes through stage matched embryos. The section planes (indicated in each figure) were carefully selected considering landmarks in all orientations within the 3D object.

Acknowledgements:

This work was supported entirely by Science Foundation Ireland (Programme Award 02/IN1/B267). We thank several members of the Edinburgh Mouse Atlas Project for helpful discussion, advice, software and assistance with its use, particularly Richard Baldock, Bill Hill and Peter Stevenson. We thank Harris Morrison for advice with running and troubleshooting OPT.

References

Barrow, J.R., Thomas, K.R., Boussadia-Zahui, O., Moore, R., Kemler, R., Capecchi, M.R. and McMahon, A.P. (2003) Ectodermal Wnt3/beta-catenin signaling is required for the establishment and maintenance of the apical ectodermal ridge. Genes Dev 17, 394-409.

Begbie, J., Brunet, J.F., Rubenstein, J.L. and Graham, A. (1999) Induction of the epibranchial placodes. Development 126, 895-902.

Brugmann, S.A., Goodnough, L.H., Gregorieff, A., Leucht, P., Ten Berge, D., Fuerer, C., Clevers, H., Nusse, R. and Helms, J.A. (2007) Wnt signaling mediates regional specification in the vertebrate face. Development 134, 3283-95.

Carroll, T.J., Park, J.S., Hayashi, S., Majumdar, A. and McMahon, A.P. (2005) Wnt9b plays a central role in the regulation of mesenchymal to epithelial transitions underlying organogenesis of the mammalian urogenital system. Dev Cell 9, 283-92.

Clevers, H. (2006) Wnt/beta-catenin signalling in Development and Disease. Cell 127, 469-480.

Couly, G., Creuzet, S., Bennaceur, S., Vincent, C. and Le Douarin, N.M. (2002) Interactions between Hox-negative cephalic neural crest cells and the foregut endoderm in patterning the facial skeleton in the vertebrate head. Development 129, 1061-73.

Crossley, P.H. and Martin, G.R. (1995) The mouse Fgf8 gene encodes a family of polypeptides and is expressed in regions that direct outgrowth and patterning in the developing embryo. Development 121, 439-51.

Francis-West, P., Ladher, R., Barlow, A. and Graveson, A. (1998) Signalling interactions during facial development. Mech Dev 75, 3-28.

Galceran, J., Farinas, I., Depew, M.J., Clevers, H. and Grosschedl, R. (1999) Wnt3a-/--like phenotype and limb deficiency in Lef1(-/-)Tcf1(-/-) mice. Genes Dev 13, 709-17.

Gorlin, R., Cohen, M. and Hennekam, R. (2001) Syndromes of the head and neck. Oxford University Press, New York.

Graham, A. (2001) The development and evolution of the pharyngeal arches. J Anat 199, 133-41.

Graham, A., Begbie, J. and McGonnell, I. (2004) Significance of the cranial neural crest. Dev Dyn 229, 5-13.

Graham, A. and Smith, A. (2001) Patterning the pharyngeal arches. Bioessays 23, 54-61.

Grammatopoulos, G.A., Bell, E., Toole, L., Lumsden, A. and Tucker, A.S. (2000) Homeotic transformation of branchial arch identity after Hoxa2 overexpression. Development 127, 5355-65.

Helms, J.A., Cordero, D. and Tapadia, M.D. (2005) New insights into craniofacial morphogenesis. Development 132, 851-61.

Hunt, P., Gulisano, M., Cook, M., Sham, M.H., Faiella, A., Wilkinson, D., Boncinelli, E. and Krumlauf, R. (1991) A distinct Hox code for the branchial region of the vertebrate head. Nature 353, 861-4.

Israsena, N., Hu, M., Fu, W., Kan, L. and Kessler, J.A. (2004) The presence of FGF2 signaling determines whether beta-catenin exerts effects on proliferation or neuronal differentiation of neural stem cells. Dev Biol 268, 220-31.

Jiang, R., Bush, J.O. and Lidral, A.C. (2006) Development of the upper lip: morphogenetic and molecular mechanisms. Dev Dyn 235, 1152-66.

Juriloff, D.M., Harris, M.J., McMahon, A.P., Carroll, T.J. and Lidral, A.C. (2006) Wnt9b is the mutated gene involved in multifactorial nonsyndromic cleft lip with or without cleft palate in A/WySn mice, as confirmed by a genetic complementation test. Birth Defects Res A Clin Mol Teratol 76, 574-9.

Lumsden, A. and Keynes, R. (1989) Segmental patterns of neuronal development in the chick hindbrain. Nature 337, 424-8.

Maden, M., Gale, E., Kostetskii, I. and Zile, M. (1996) Vitamin A-deficient quail embryos have half a hindbrain and other neural defects. Curr Biol 6, 417-26.

McGonnell, I.M., Clarke, J.D. and Tickle, C. (1998) Fate map of the developing chick face: analysis of expansion of facial primordia and establishment of the primary palate. Dev Dyn 212, 102-18.

Minkoff, R. (1980) Regional variation of cell proliferation within the facial processes of the chick embryo: a study of the role of 'merging' during development. J Embryol Exp Morphol 57, 37-49.

Minkoff, R. (1991) Cell proliferation during formation of the embryonic facial primordia. J Craniofac Genet Dev Biol 11, 251-61.

Murphy, P., Davidson, D.R. and Hill, R.E. (1989) Segment-specific expression of a homoeobox-containing gene in the mouse hindbrain. Nature 341, 156-9.

Murphy, P. and Hill, R.E. (1991) Expression of the mouse labial-like homeobox-containing genes, Hox 2.9 and Hox 1.6, during segmentation of the hindbrain. Development 111, 61-74.

Niemann, S., Zhao, C., Pascu, F., Stahl, U., Aulepp, U., Niswander, L., Weber, J.L. and Muller, U. (2004) Homozygous WNT3 mutation causes tetra-amelia in a large consanguineous family. Am J Hum Genet 74, 558-63.

Noden, D.M. (1986) Origins and patterning of craniofacial mesenchymal tissues. J Craniofac Genet Dev Biol Suppl 2, 15-31.

Oosterwegel, M., van de Wetering, M., Timmerman, J., Kruisbeek, A., Destree, O., Meijlink, F. and Clevers, H. (1993) Differential expression of the HMG box factors TCF-1 and LEF-1 during murine embryogenesis. Development 118, 439-48.

Schneider, R.A. and Helms, J.A. (2003) The cellular and molecular origins of beak morphology. Science 299, 565-8.

Sharpe, J., Ahlgren, U., Perry, P., Hill, B., Ross, A., Hecksher-Sorensen, J., Baldock, R. and Davidson, D. (2002) Optical projection tomography as a tool for 3D microscopy and gene expression studies. Science 296, 541-5.

Shu, W., Guttentag, S., Wang, Z., Andl, T., Ballard, P., Lu, M.M., Piccolo, S., Birchmeier, W., Whitsett, J.A., Millar, S.E. and Morrisey, E.E. (2005) Wnt/beta-catenin signaling acts upstream of N-myc, BMP4, and FGF signaling to regulate proximal-distal patterning in the lung. Dev Biol 283, 226-39.

Soshnikova, N., Zechner, D., Huelsken, J., Mishina, Y., Behringer, R.R., Taketo, M.M., Crenshaw, E.B., 3rd and Birchmeier, W. (2003) Genetic interaction between Wnt/beta-catenin and BMP receptor signaling during formation of the AER and the dorsal-ventral axis in the limb. Genes Dev 17, 1963-8.

Summerhurst K., Stark M., Sharpe J., Davidson D. and P., Murphy. (2008) 3D representation of of Wnt and Frizzled gene expression patterns in the mouse embryo at embryonic day 11.5 (Ts 19). Gene Expression Patterns 8, 331-48.

Torres, M.A., Eldar-Finkelman, H., Krebs, E.G. and Moon, R.T. (1999) Regulation of ribosomal S6 protein kinase-p90(rsk), glycogen synthase kinase 3, and beta-catenin in early Xenopus development. Mol Cell Biol 19, 1427-37.

Trainor, P.A. and Krumlauf, R. (2000) Patterning the cranial neural crest: hindbrain segmentation and Hox gene plasticity. Nat Rev Neurosci 1, 116-24.

Veitch, E., Begbie, J., Schilling, T.F., Smith, M.M. and Graham, A. (1999) Pharyngeal arch patterning in the absence of neural crest. Curr Biol 9, 1481-4.

Wedden, S.E. (1987) Epithelial-mesenchymal interactions in the development of chick facial primordia and the target of retinoid action. Development 99, 341-51.

Wendling, O., Dennefeld, C., Chambon, P. and Mark, M. (2000) Retinoid signaling is essential for patterning the endoderm of the third and fourth pharyngeal arches. Development 127, 1553-62.

Wilkinson, D.G., Bhatt, S., Cook, M., Boncinelli, E. and Krumlauf, R. (1989) Segmental expression of Hox-2 homoeobox-containing genes in the developing mouse hindbrain. Nature 341, 405-9.

Xu, Q. and Wilkinson, D. (1998) In situ hybridisation of mRNA with hapten labelled probes. In Wilkinson, D.G. (ed.), In Situ Hybridisation: A Practical Approach, 2nd edition, Oxford University Press, Oxford, pp. 87-106.

Young, D.L., Schneider, R.A., Hu, D. and Helms, J.A. (2000) Genetic and teratogenic approaches to craniofacial development. Crit Rev Oral Biol Med 11, 304-17.

Figure legends

Fig. 1: External views of 3D representations of OPT reconstructions of the expression patterns of Lef1, Tcf1, Tcf3. Tcf4 and β-catenin across ages of development E9.5, E10.5 and E11.5. Since expressing / stained tissues in the embryos have greater optical density, they appear as white/light grey against a dark background of unstained regions. Scale bars 1mm.

Fig. 2: Photomicrographs of in situ hybridised embryos prior to OPT scanning, focusing on the facial region. Ages and probes as indicated. This shows the level of detail visible from such superficial views. Scale bars 1mm.

Fig. 3: Comparison of sagittal sections through 3D reconstructions representing expression of Tcf/Lef family and β-catenin genes in the facial primordia at E9.5. A shows an external view of a 3D reconstruction (showing expression of Lef1) with the frontonasal process (Fp), maxillary (Mx) and mandibular (Mn) components of the 1st branchial arch, 2nd and 3rd branchial arches indicated. B represents the planes of section shown in rows 1 and 2 of 3D reconstructions of each of the 5 gene expression patterns (as indicated). Scale as in Figure 1

Fig. 4: Comparison of transverse sections through 3D reconstructions representing expression of Tcf/Lef family and β-catenin genes in the facial primordia at E9.5. A indicates the planes of section shown in the images above, through the maxillary

component (a; Mx) of the 1st branchial arch, the frontonasal process (b; Fp), the mandibular (Mn) component of the 1st and the 2nd branchial arch (c and d) and through the 3rd branchial arch (e). Scale as in Figure 1

Fig. 5: Comparison of coronal sections through 3D reconstructions representing expression of Tcf/Lef family and β-catenin genes in the facial primordia at E9.5. A indicates the planes of section shown in the images above, through the frontonasal process (a; Fp), maxillary and mandibular components (b and c; Mx and Mn) of the 1st branchial arch, and the 2nd and 3rd branchial arches (c and d). Scale as in Figure 1.

Fig. 6: Comparison of external views (row 1) and sagittal sections (row 2) through 3D reconstructions representing expression of Tcf/Lef family and β-catenin genes in the facial primordia at E10.5. A shows an external view of a 3D reconstruction (showing expression of Tcf1) with the frontonasal process (Fp), maxillary (Mx) and mandibular (Mn) components of the 1st branchial arch, 2nd and 3rd and 4th branchial arches indicated. B represents the aspect viewed in row 1 (arrow, from the left) and the plane of section shown in row 2 for 3D reconstructions of each of the 5 gene expression patterns (as indicated). Scale as in Figure 1.

Fig. 7: Comparison of transverse sections through 3D reconstructions representing expression of Tcf/Lef family and β-catenin genes in the facial primordia at E10.5. A indicates the planes of section shown in the images above, through the frontonasal process and maxillary component of the 1st branchial arch (a; Mx Fp), the mandibular (Mn) component of the 1st and the 2nd branchial arch (b and c) and through the 2nd and 3rd (d), 4th (e) and 6th (f) branchial arches. Scale as in Figure 1.

Fig. 8: Comparison of coronal sections through 3D reconstructions representing expression of Tcf/Lef family and β-catenin genes in the facial primordia at E10.5. A indicates the planes of section shown in the images above, through the frontonasal process (a; Fp), the anterior (b) and posterior (c) maxillary and mandibular components of the 1st branchial arch, the anterior of the 2nd (d) and through the 2nd, 3rd 4th and 6th branchial arches (e). Scale as in Figure 1.

Fig 9: Comparison of external views (row 1) and sagittal sections (row 2) through 3D reconstructions representing expression of Tcf/Lef family and β-catenin genes in the facial primordia at E11.5. A shows an external view of a 3D reconstruction (showing expression of Tcf1) with the frontonasal process (Fp), maxillary (Mx) and mandibular (Mn) components of the 1st branchial arch, and 2nd branchial arch indicated. B represents the side viewed in row 1 (arrow, from the left) and the plane of section shown in row 2 for 3D reconstructions of each of the 5 gene expression patterns (as indicated). Scale as in Figure 1.

Fig 10: Comparison of transverse sections through 3D reconstructions representing expression of Tcf/Lef family and β-catenin genes in the facial primordia at E11.5. A indicates the planes of section shown in the images above, through the frontonasal process (Fp), maxillary (Mx) and mandibular (Mn) components of the 1st branchial arch

(a and b), the frontonasal process, mandibular component of the 1st and 2nd branchial arches (c) and 2nd branchial arch (d). Scale as in Figure 1.

Fig 11: Comparison of coronal sections through 3D reconstructions representing expression of Tcf/Lef family and β-catenin genes in the facial primordia at E11.5. A indicates the planes of section shown in the images above, through the frontonasal process (a; Fp), the maxillary and mandibular components of the 1st branchial arch (b-d), and through the territories of the 2nd, 3rd 4th and 6th branchial arches (e). B summarises the externally visible pattern of expression of the canonical pathway reporter gene TOPgal at E11.5, shown in Brugmann et al. (2007) Figure 2. This may be broadly compared to the transcript distribution of canonical pathway transcriptional regulators shown in panels a and d bearing in mind that the data here show sections through the territories rather than external views. Scale as in Figure 1.

Table 2: Details of expression probes used to reveal specific expression.

Gene	Extent of Probe on Genbank Sequence	Probe length in nucleotides	Source
Lef1	Nucleotide 2019 to 2460 on NM_016269.3	441	J. Meeldijk
Tcf1	Nucleotide 18 to 1572 on NM_009331.3	1554	R.Grosschedl
Tcf3	Nucleotide 86 to 1582 on NM_009332.2	1496	Cloned: limb library screen
Tcf4	Nucleotide 424 to 839 on NM_009333.2	415	J.Rubenstein
β-catenin	Nucleotide 2194 to 2621 on NM_007614.2	427	U.Borello/ G. Cossu

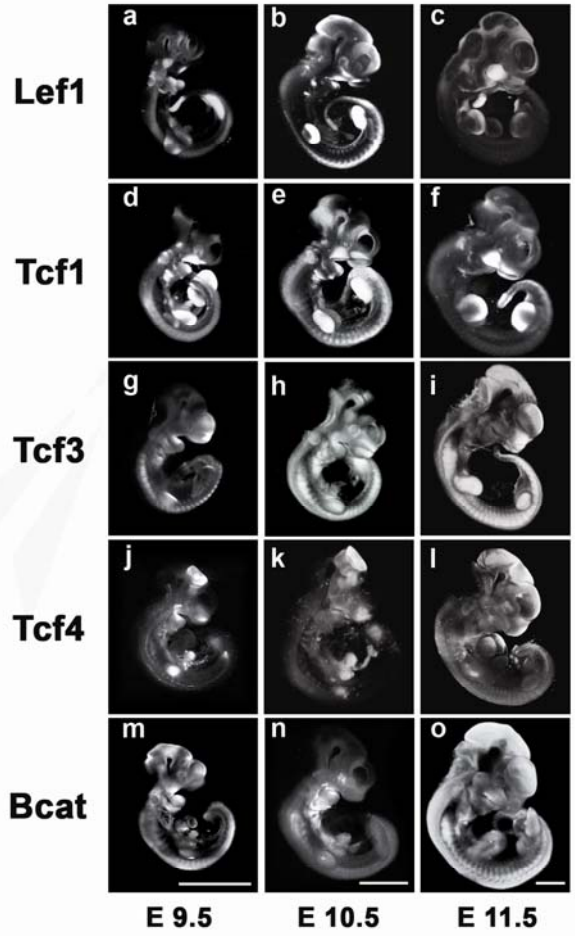

FIGURE 1

FIGURE 2

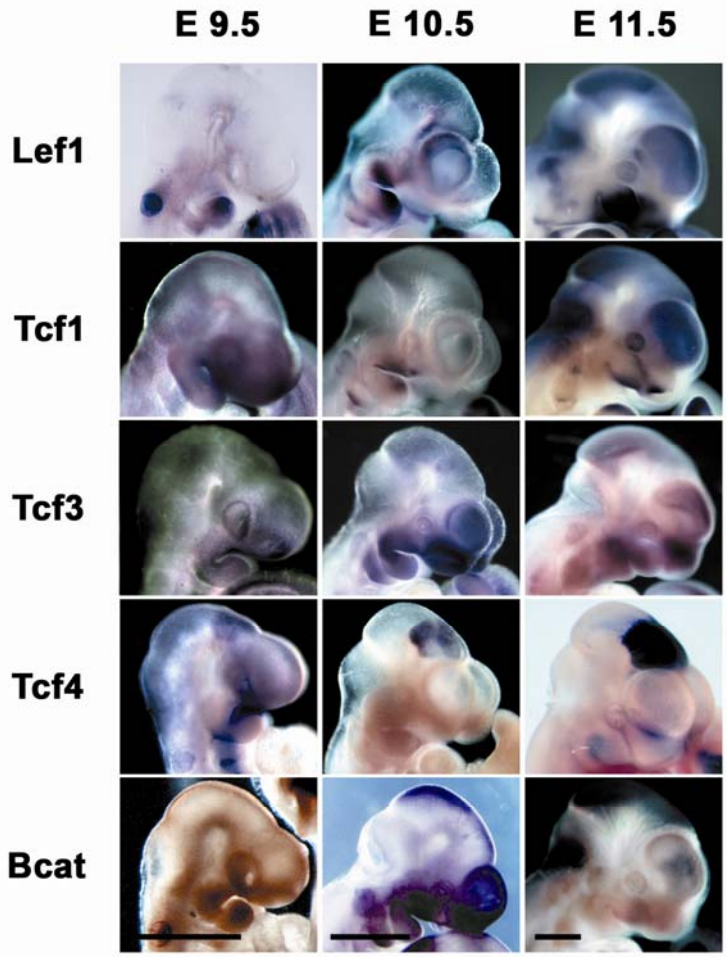

FIGURE 3

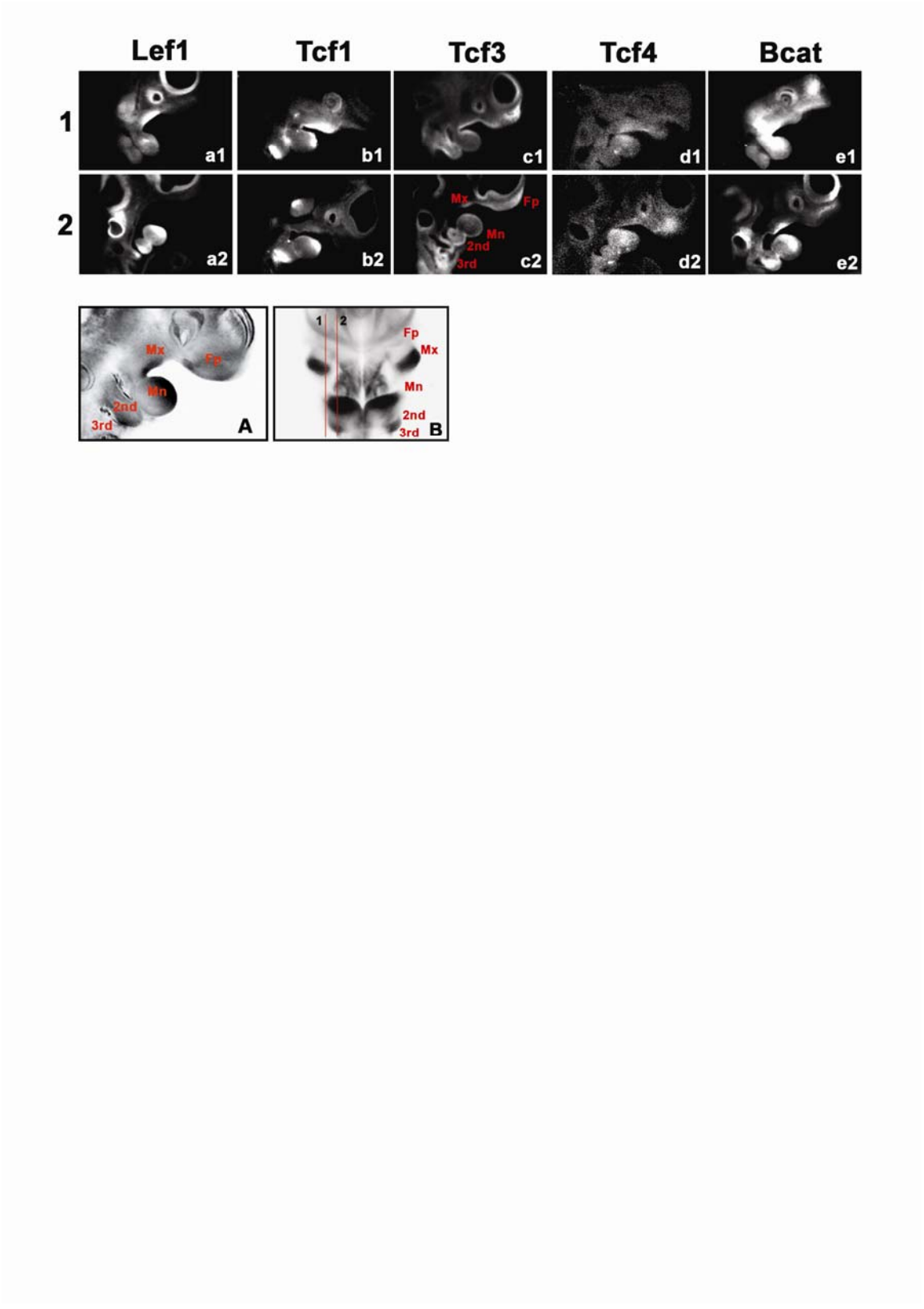

FIGURE 4

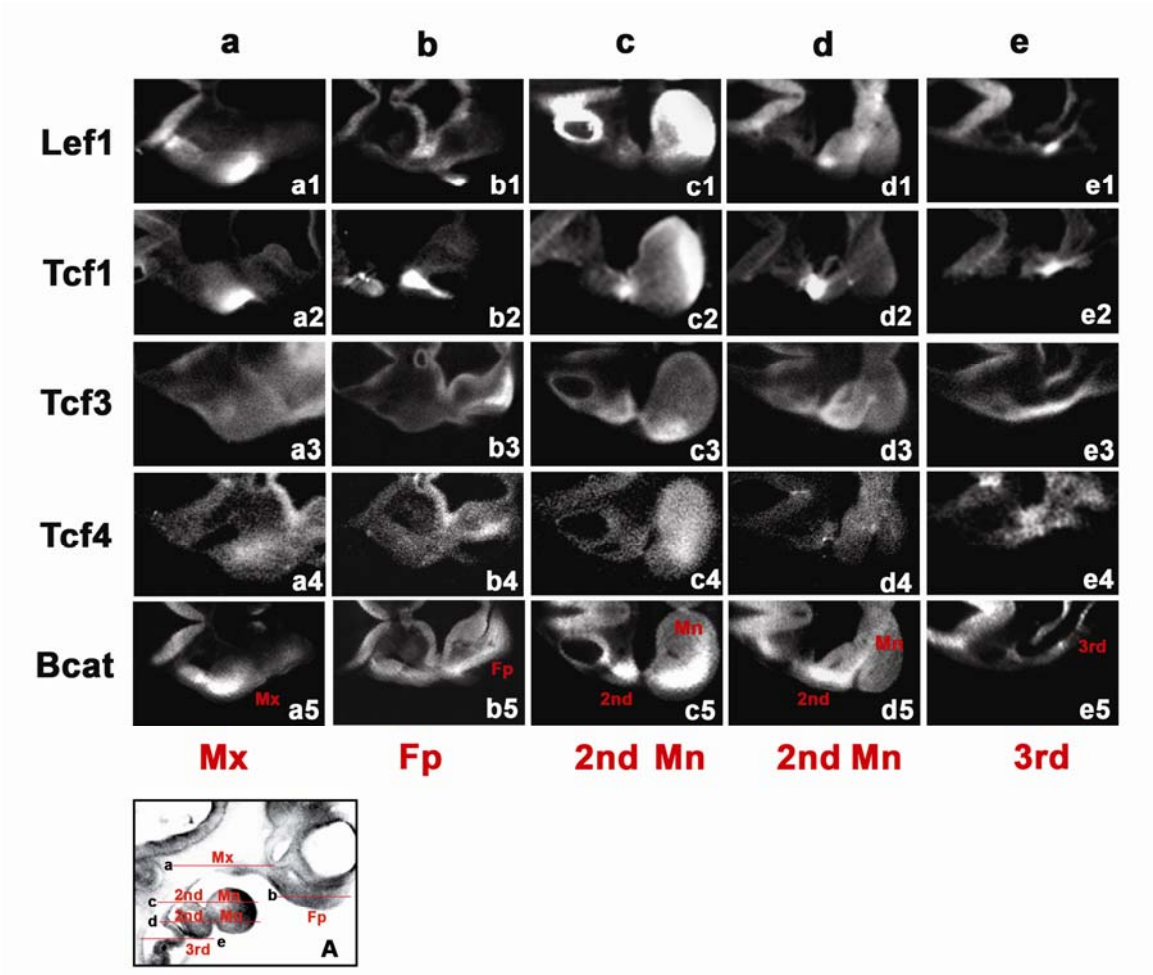
a
b
c
d
e
Lef1
Tcf1
Tcf3
Tcf4
Bcat
a1
b1
c1
d1
e1
a2
b2
c2
d2
e2
a3
b3
c3
d3
e3
a4
b4
c4
d4
e4
Mx
a5
Fp
b5
Mn
2nd
c5
Mn
2nd
d5
3rd
e5
Mx
Fp
2nd Mn
2nd Mn
3rd
Mx
2nd Mn
2nd Mn
Fp
3rd
A

FIGURE 5

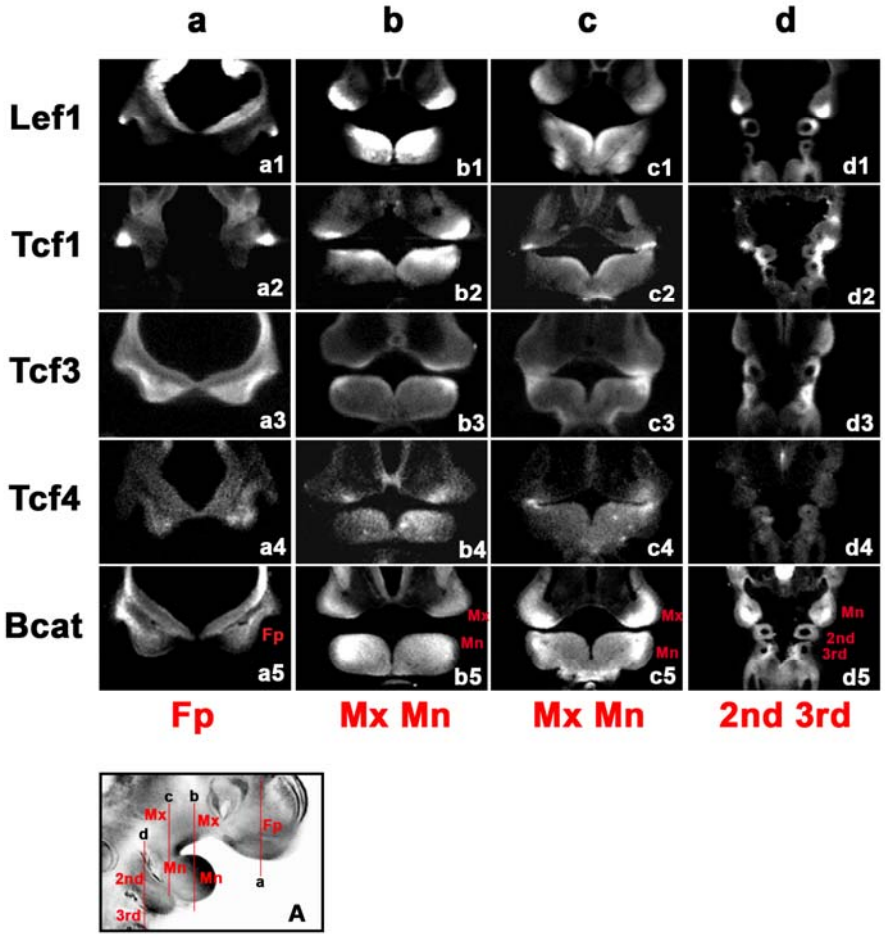

FIGURE 6

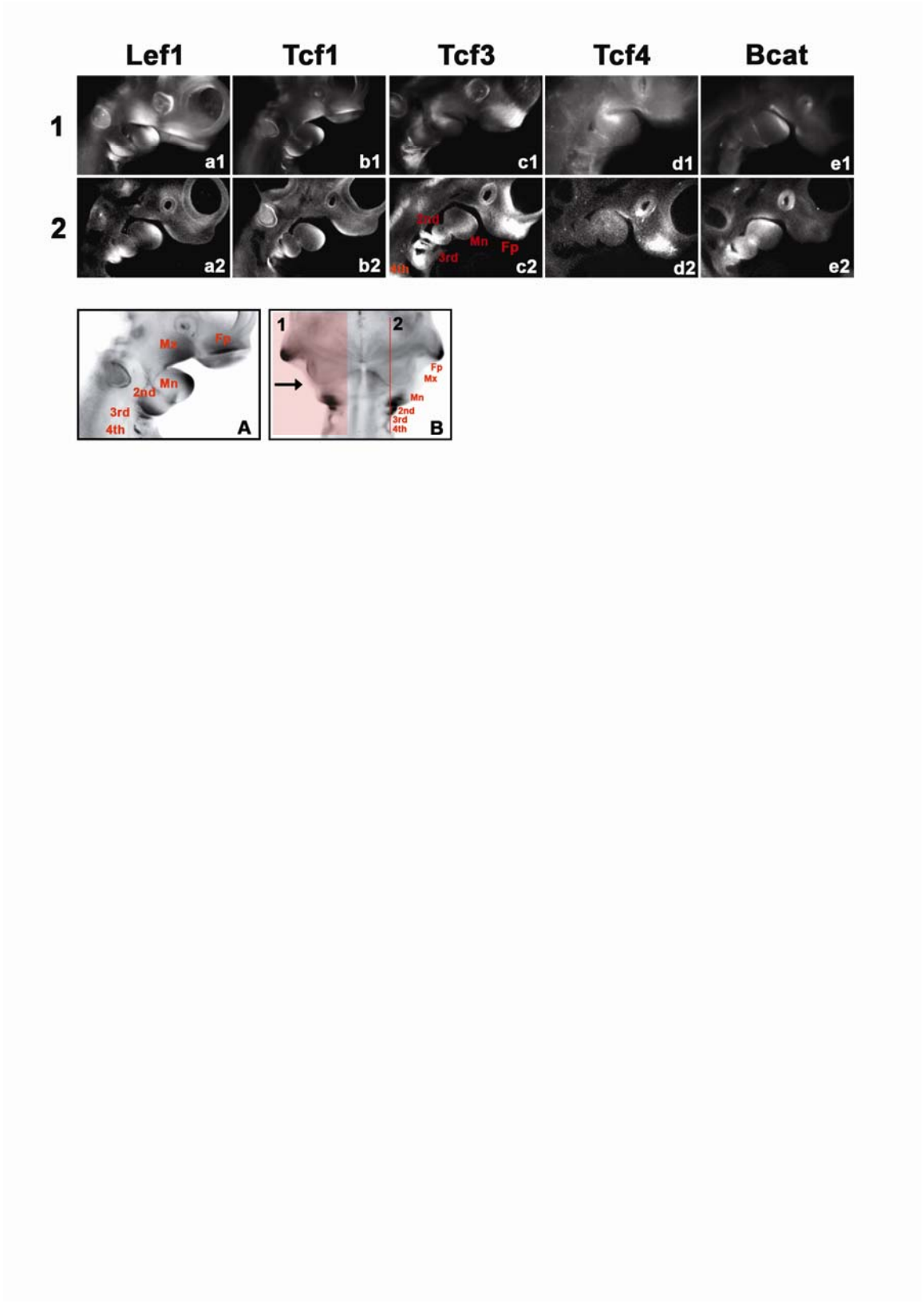

FIGURE 7

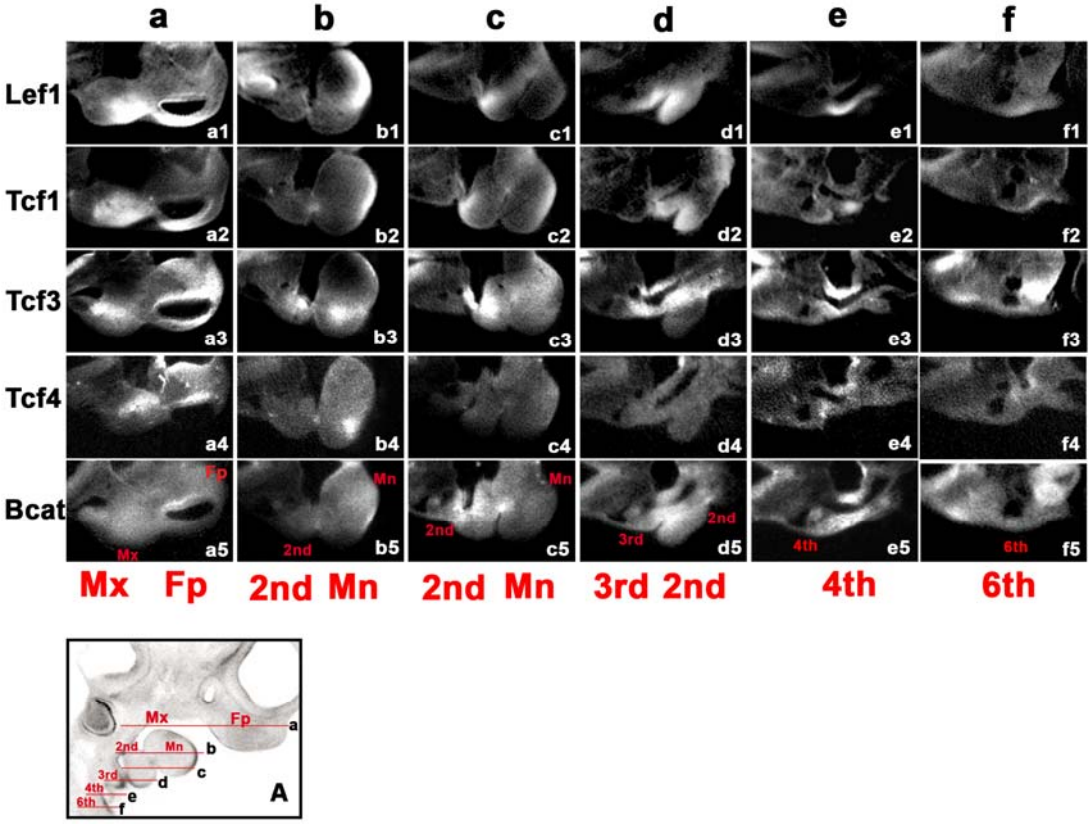

FIGURE 8

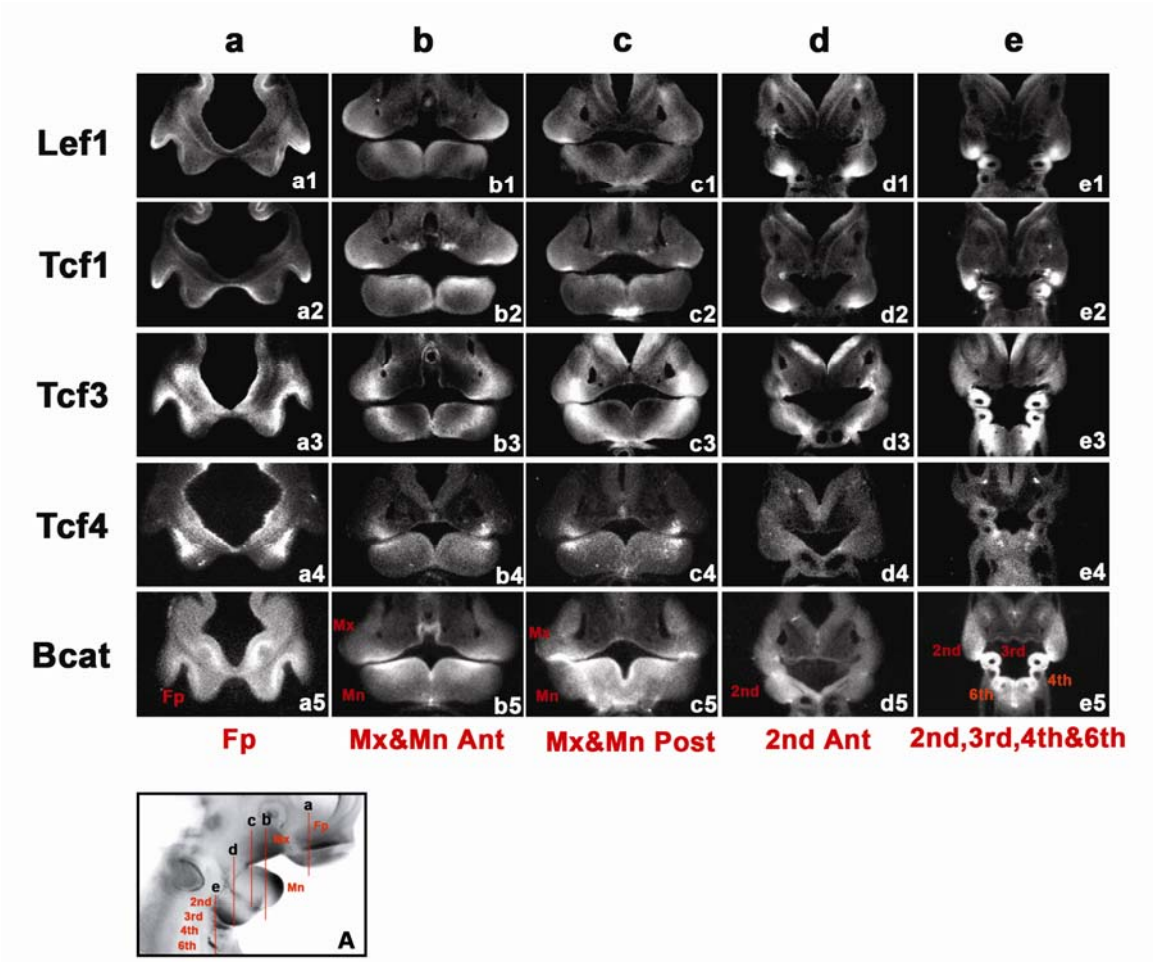
a
b
c
d
e
Lef1
Tcf1
Tcf3
Tcf4
Bcat
a1
b1
c1
d1
e1
a2
b2
c2
d2
e2
a3
b3
c3
d3
e3
a4
b4
c4
d4
e4
Fp
a5
Mx
Mn
b5
Mx
Mn
c5
2nd
d5
2nd
3rd
4th
6th
e5
Fp
Mx&Mn Ant
Mx&Mn Post
2nd Ant
2nd,3rd,4th&6th
a
b
c
d
e
Fp
Mx
Mn
2nd
3rd
4th
6th
A

FIGURE 9

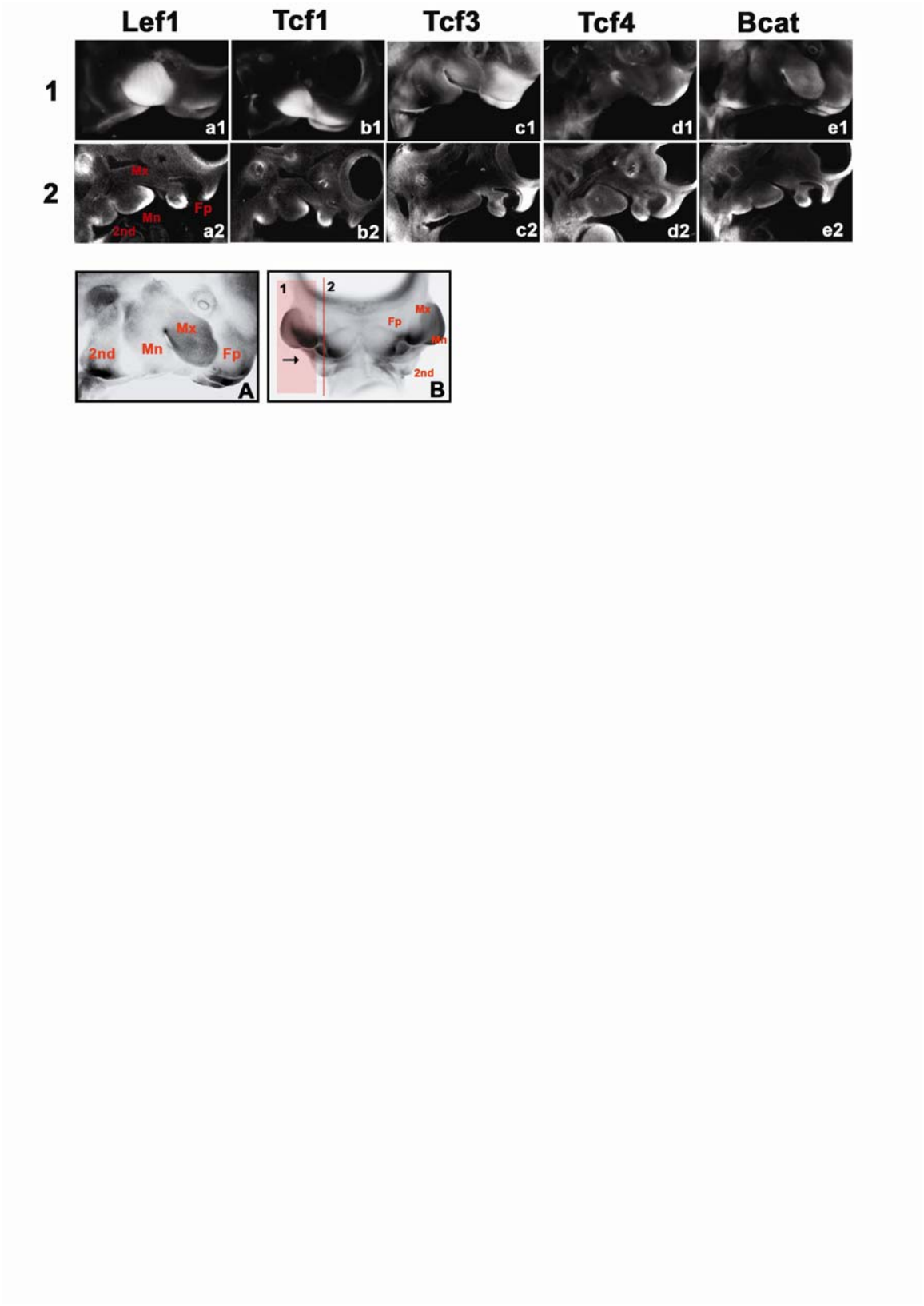

FIGURE 10

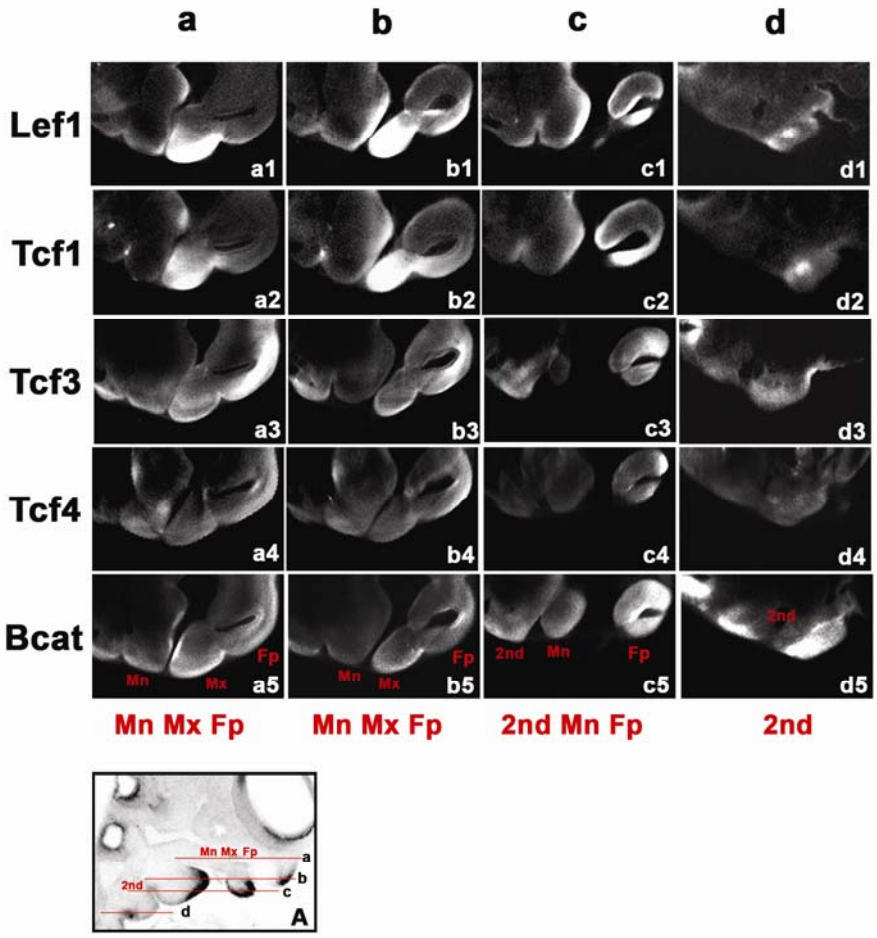

FIGURE 11

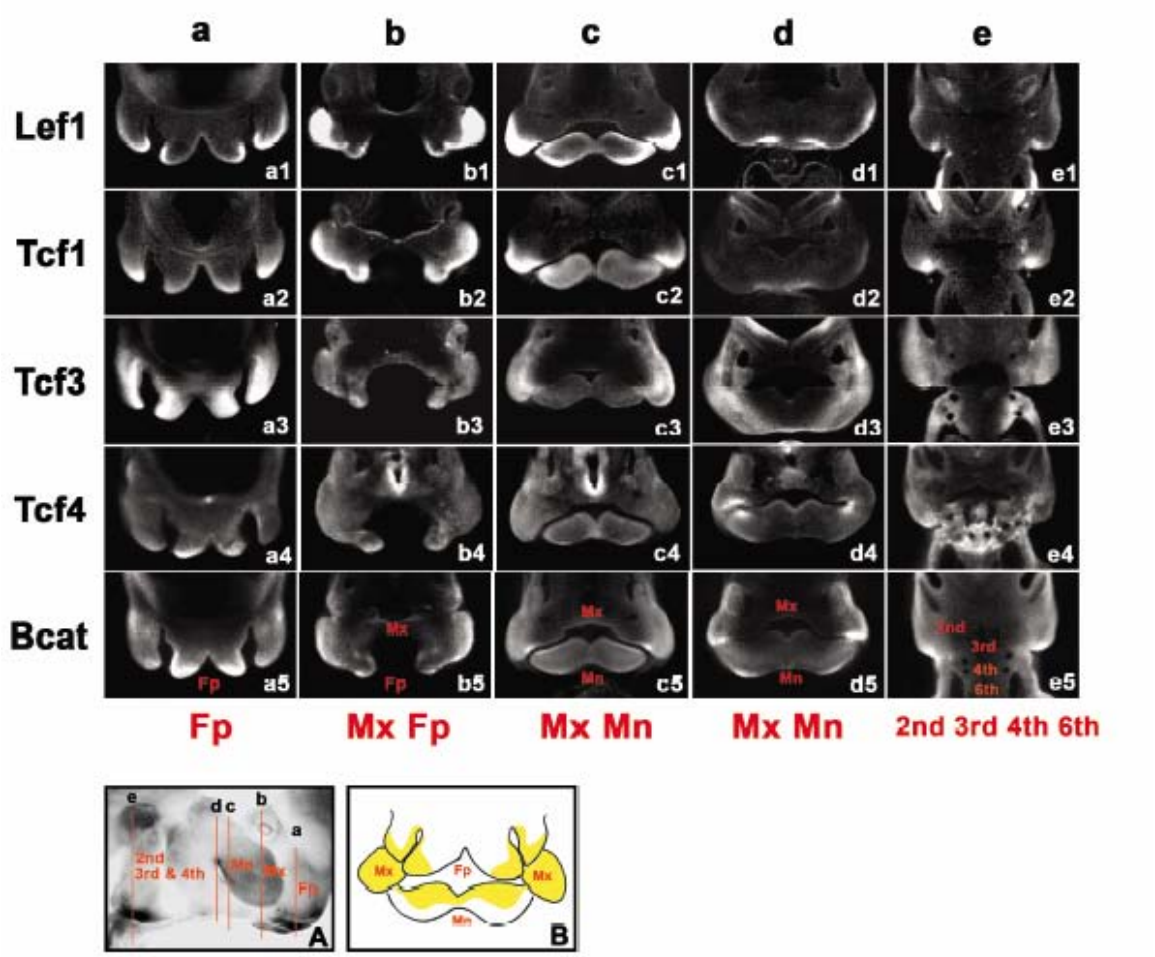

Tables

Table 1: Summary of the facial territories where Lef1, Tcf1, Tcf3, Tcf4 and β-catenin are expressed (green indicates expression; red indicates no expression) and reference to the figure panels where the spatial distribution in these territories can be directly compared. Abbreviations: Fnp, frontonasal process; Max, the maxillary and Mand, the mandibular components of the 1st branchial arch; 2nd, 3rd 4th and 6th, the appropriate branchial arche. Note the 6th branchial arch is not yet visible at E9.5.

Lef1

	Fnp	1st Max	1st Mand	2nd	3rd	4th	6th
E9.5	lateral		rostro-medial	caudo-lateral	rostro-lateral		NA
	Fig: **4**b1,**5**a1	Fig: **3**a1, **4**a1, **5**b1,c1	Fig: **3**a2, **4**c1, **5**b1,c1	Fig: **3**a2, **4**d1, **5**c1,d1	Fig: **3**a2, **5**d1	Fig: **5**d1	
E10.5							
	Fig: **6**a1, **7**a1, **8**a1	Fig: **6**a1, **7**a1, **8**b1,c1	Fig: **6**a1,a2, **7**b1, **8**b1,c1	Fig: **6**a1,a2, **7**c1,d1, **8**d1,e1	Fig: **7**d1, **8**e1,d1	Fig: **7**e1, **8**e1	
E11.5							
	Fig:**9**a1,a2,**10**b1,c1, **11**a1,b1	Fig: **9**a1, **10**a1,b1, **11**b1,c1	Fig:**9**a2, **10**a1,b1,c1,**11**c1,d1	Fig: **9**a2, **10**d1, **11**e1			

Tcf1

E9.5							NA
	Fig: **5**a2, **4**b2	Fig: **3**b1, **4**a2, **5**b2, c2	Fig: **3**b1,b2, **4**c2, **5**b2,c2	Fig: **3**b1,b2**,** **4**c2,d2, **5**d2	Fig: **5**d2	Fig: **5**d2	
E10.5							
	Fig: **6**b1,b2, **7**a2, **8**a2	Fig: **6**b2, **7**a1, **8**b2,c2	Fig: **6**b1,b2, **7**b2,c2, **8**b2,c2	Fig: **6**b1,b2, **7**c2,d2, **8**d2,e2	Fig: **6**b1,b2, **7**d2, **7**e2	Fig: **6**b1,b2, **7**e2, **8**e2	
E11.5							
	Fig: **8**b1,b2, **10**c2	Fig: **9**b1, **10**a2,b2, **11**b2,c2	Fig: **9**b2,**10**a1,b1,c1,**11**c2,d2	Fig: **9**b2, **10**d2, **11**e2			

Tcf3

E9.5							NA
	Fig: **3**c2, **4**b3**,** **5**a3	Fig: **3**c1, **4**a3, **5**b3	Fig: **3**c2, **4**c3,d3, **5**b3,c3	Fig: **3**c1,c2, **4**c3,d3, **5**d3	Fig: **3**c2, **5**d3	Fig: **3**c2, **5**d3	
E10.5							
	Fig: **6**c1,c, **7**a3, **8**a3	Fig: **6**c1, **7**a3 , **8**b3,c3	Fig: **6**c1,c2, **7**b3,c3, **8**b3,c3	Fig: **6**c1,c2 **7**b3,c3, **8**d3,e3	Fig: **6**c1,c2, **7**d3, **8**e3	Fig: **6**c1,c2, **7**e3, **8**e3	Fig: **8**e3
E11.5							X
	Fig:**9**c1,c2, **10**a3,b3,**11**a3,b3	Fig: **9**c1, **10**a3,b3, **11**c3	Fig: **9**c1, **11**d3	Fig: **10**d3, **11**e3	Fig: **11**e3	Fig: **11**e3	

Tcf4

E9.5							NA
	Fig: **3**d1, **4**b, **5**a4	Fig: **3**d2, **4**a4, **5**b4,c4	Fig **3**d1,d2, **4**c4, **5**b4,c4				
E10.5						very low	
	Fig: **6**d2, **7**a4 **,** **8**a4	Fig: **6**d1, **7**a4 **,** **8**b4,c4	Fig: **6**d1, **7**b2, **8**b4,c4	Fig: **6**d2, **7**c4, **8**d4,e4	Fig: **7**d4, **8**e4	Fig: **7**e4, **8**e4	
E11.5				very low			
	Fig: **9**d1, **10**a4,b4,c4, **11**a4	Fig: **9**d1, **11**d4	Fig: **9**d1, 10a4, 11d4	Fig: **10**d4, 11e4	Fig: **11**e4	Fig: **11**e4	Fig: **11**e4

β-catenin

E9.5							NA
	Fig: **3**e2, **4**b5**,** **5**a5	Fig: **3**e1,e2**,** **4**a5,**5**b5,c5	Fig: **3**e1,e2**,** **4**c5, **5**b5,c5	Fig: **3**e2, **4**c5,d5, **5**d5	Fig: **5**d5	Fig: **5**d5	
E10.5							
	Fig: **6**e1**,** **7**a5, **8**a5	Fig: **6**e1,e2**,** **7**a5, **8**b5,c5	Fig: **6**e1,e2**,** **7**b5, **8**b5,c5	Fig: **6**e2**,** **7**c5,d5, **8**d5,e5	Fig: **6**e2**,** **7**d5, **8**e5	Fig: **7**e5**,** **8**e5	Fig: **8**e5
E11.5							
	Fig: **9**e1,e2**,** **10**b5,c5, **11**a5	Fig: **9**e1**,** **10**a5,b5, **11**c5,d5	Fig: **9**e2**,** **11**c5	Fig: **9**e1,e2**,** **10**d5			